Vol 14 No 8, August 2005
1009-1963/2005/14(08)/1626-05
Chinese Physics
© 2005 Chin. Phys. Soc.
and IOP Publishing Ltd

Surface morphology evolution of Si(110) by ion sputtering as a function of sample temperature*

Qi Le-Jun(漆乐俊)[a], Ling Li(凌 立)[b], Li Wei-Qing(李维卿)[a],
Yang Xin-Ju(杨新菊)[c], Gu Chang-Xin(顾昌鑫)[b], and Lu Ming(陆 明)[a]†

[a] *Department of Optical Science and Engineering, and State Key Laboratory for Advanced Photonic Materials and Devices, Fudan University, Shanghai 200433, China*

[b] *Department of Materials Science, Fudan University, Shanghai 200433, China*

[c] *Surface Physics Laboratory, Fudan University, Shanghai 200433, China*

(Received 19 December 2004; revised manuscript received 28 March 2005)

Si(110) surface morphology evolution under normal-incident Ar^+ ion sputtering has been studied as a function of Si temperature with the ion energy of 1.5keV and the ion flux 20μA/cm^2. During temperature rising from room temperature to 800°C, Si(110) surface morphology changes from a dim dot/hole pattern to a distinct dot one, meanwhile the surface roughness increases steadily. The usually-accepted Bradley–Harper model fails to explain these data. By taking into account the Ehrlich–Schwoebel effect in the nanostructuring process, a simulation work was conducted based on a continuum dynamic model, which reproduces the experimental results.

Keywords: sputtering, surface diffusion, silicon, nanostructuring, models of nonlinear phenomena
PACC: 6820, 6180, 6185, 6822

1. Introduction

Nanostructuring of solid surfaces by inert ion sputtering has attracted considerable attention in recent years due to the effectiveness of this technique in producing spatially dense nanodot arrays.[1–8] In the meanwhile, theoretical models have been proposed, modified and refined aiming to disclose the physics underlying this novel nanostructuring phenomenon.[9–12] At present, the Bradley–Harper (BH) model[8–10] has been regarded as valid to describe the nanostructuring of semiconductor single-crystals, while the Ehrlich–Schwoebel (ES) model[7,8,12] is good for metals. Our recent work on Si(100)[13] reveals, however, that both mechanisms may be operative during nanostructuring of all the solid targets, and the ion flux plays a critical role in determining which model predominates in the process. In this work, nanostructuring of Si(110) as a function of the sample temperature has been studied under the condition of normal-incident Ar^+ ion sputtering and low ion flux (20μA/cm^2). It is found that a distinct dot pattern forms on Si(110) at elevated temperatures, and with increasing temperature, both the dot size and the surface roughness increase. These results are not consistent with the BH model usually accepted as good for semiconductors. By taking into account the ES effect in the nanostructuring process, a continuum dynamic model[11] has been adopted, which reproduces the surface morphology and the surface roughness evolutions in a qualitative manner.

2. Experiments

Si(110) wafers (p-type, 1–10Ωcm) were firstly degreased in the solution of 95%–98% H_2SO_4 and 30% H_2O_2 with a ratio of 1:1 at the boiling temperature for 5 min. They were then rinsed thoroughly with distilled water, and supersonically cleaned in acetone and alcohol in sequence. After dried in air, Si was transferred into the vacuum chamber of a home-built ion sputtering system. A Perkin-Elmer sputtering gun (model 04-303) was used for sputtering. The incident ion beam was normal to the Si surface. Prior to sputtering, the Ar^+ ion flux was measured with a Faraday

*Project supported by the National Natural Science Foundation of China (Grant No 10374016), and the Science and Technology Commission of Shanghai (Grant No 03DJ14001).
†E-mail: minglu@fudan.ac.cn

cup located above the sample holder. The ion flux was $20\mu A/cm^2$ with an ion energy 1.5keV. The base pressure of the chamber was 5×10^{-7}Pa, and during sputtering, the pressure rose up to $\sim5\times10^{-5}$Pa. Sample heating was accomplished through biased electron-beam-bombardment at the backside of the sample. The temperature was measured with a calibrated thermocouple. The temperature ranged from room temperature (RT) to 800°C. The Ar^+ dose was 5×10^{17} ions/cm^2, which is equivalent to ~100 monolayers of Si removed after ion sputtering as estimated by the TRIM software.[14] Surface morphology was measured *ex situ* with an ambient atomic force microscope (AFM), model Solver P47 of NT-MDT, at RT in contact mode.

3. Results and discussion

3.1. Operation of the Ehrlich-Schwoebel mechanism

In Figs.1(a)–(d), typical AFM images for the sputtered Si(110) surfaces are presented; the sample temperatures are RT, 500, 600 and 800°C, respectively. Before ~600°C, the surface morphology is characterized by a dim dot/hole pattern (Figs.1.(a), (b)). However, for temperature $\geq$ ~600°C, a distinct dot pattern appears (Figs.1 (c), (d)), and the average dot size increases with increasing temperature. Ion sputtering alone (without heating the sample) cannot yield this surface morphology (Fig.1(a)), neither can heating the Si(110) alone (not shown here). A synergetic effect between ion energy and sample temperature then exists for the formation of the dot pattern on Si(110), which is similar to the case of MgO(100).[6]

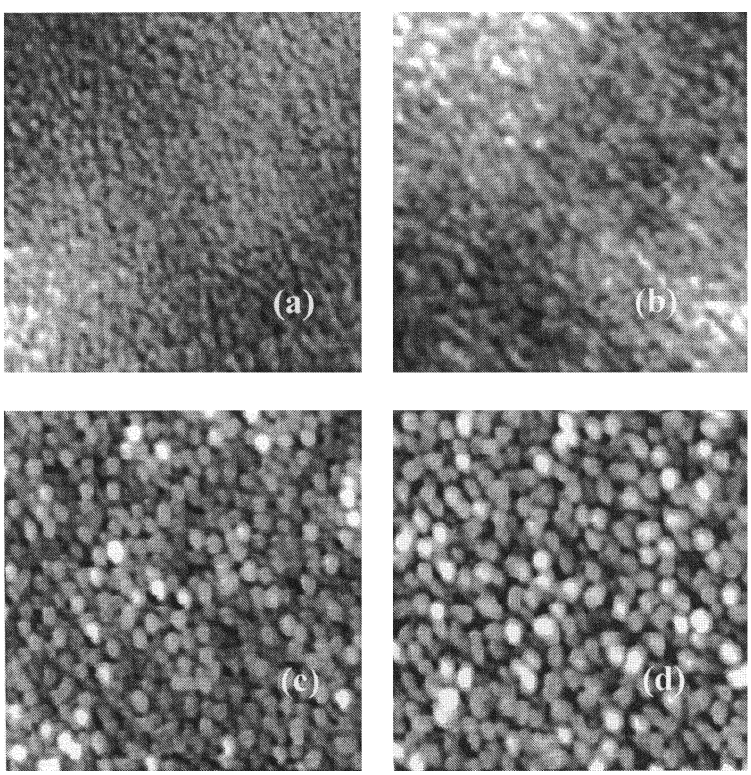


Fig.1. AFM images of Si(110) after Ar^+ ion sputtering, with ion energy =1.5keV, ion dose =5×10^{17} ions/cm^2, ion flux =$20\mu A/cm^2$, and sample temperature T=RT (a); 500°C (b); 600°C (c) and 800°C (d). The image size is 800 nm×800nm for all figures.

Figure 2(a) plots the measured root-mean-square surface roughness, w, versus sample temperature, T, for the sputtered Si(110). Initially, w rises slowly with rising T, then beyond ~500°C, it starts to increase quickly; after reaching a maximum point, w shows a sign of tendency to fall. The quick increase in w is coincident with the appearance of the distinct dot pattern. The surface morphology evolution is not consistent with the BH model as the ion collision process is insensitive to the sample temperature;[14] neither is the w-T relationship since the BH model predicts a steady decrease of surface roughness with increasing T.[4] The measured w-T relationship is, however, in agreement with the ES model.[7,12] The ES diffusivity

depends on three factors. The first one is the rebounding probability of adatoms (vacancies) at the step edge due to step edge barrier (ES barrier), which is proportional to $1 - \exp(-E_{\rm ES}/kT)$, where $E_{\rm ES}$ stands for the ES barrier, and k the Boltzmann constant. This probability alone cannot guarantee the deposited adatoms (vacancies) on terraces to fulfill a biased uphill (downhill) ES diffusion; a prerequisite for the ES diffusion is that the adatoms (vacancies) should be located in the acting region of the rebounding force due to the ES barrier. This results in the second factor, i.e. the migrating probability on terrace, which is proportional to $\exp(-E_0/kT)$, where E_0 is the activation energy for thermal or ion-induced diffusion. The third one is related to the up-climbing (down-slipping) of adatoms (vacancies) at the step edges, whose probability is $\sim \exp(-E_1/kT)$, where E_1 is the energy barrier for the step climbing. With increasing T, the first probability falls while the latter two rise. The product of these three probabilities is presumably proportional to the ES diffusivity, and changes with temperature in a bell-shape-like manner as sketched in Fig.3. This behaviour leads to the w-T evolution as shown in Fig.2(a). For previously studied metal single-crystals under the low flux ion sput tering,[7,8] bell-shape-like relationships for w-T have always been observed. It has been established that in these cases, the ES model dominates the nanostructuring process. Therefore in the following simulations, the ES effect is mainly considered, and the contribution from the BH one is taken as a minor constant.

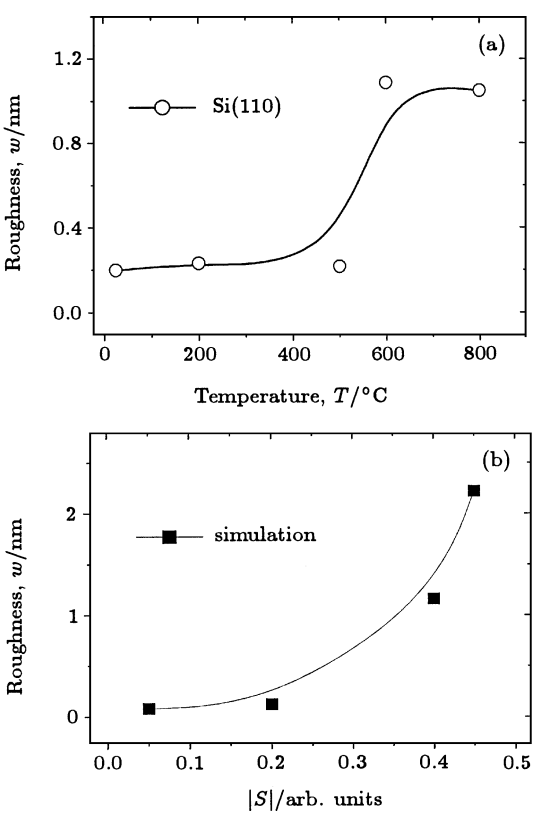


Fig.2. (a) The measured surface roughness versus sample temperature; (b) the calculated surface roughness versus S (the ES diffusivity).

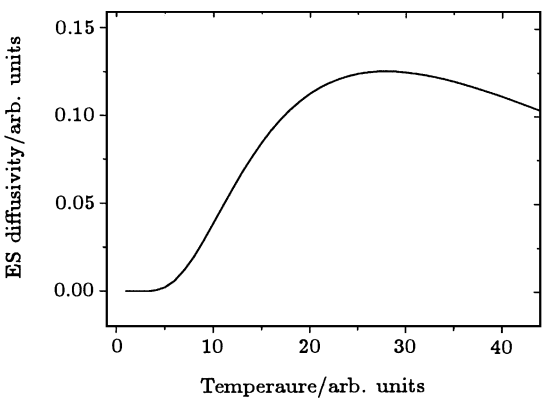


Fig.3. Sketch for the evolution of the ES diffusivity versus T.

3.2. Simulations based on a continuum model

Rusponi *et al*[11] have proposed a continuum dynamic model that actually combines the BH and ES effects together, which reads

$$\partial h/\partial t = \sum_n \{(-\nu_n - S_n)\partial^2 h/\partial \boldsymbol{n}^2 + (\partial h/\partial \boldsymbol{n})^2 \lambda_n/2 - D_n \partial^4 h/\partial \boldsymbol{n}^4\} + \eta(x,y,t), \quad (1)$$

where $h(x,y,t)$ is the height of a position (x,y) on the surface at time of t; $\boldsymbol{n}$ stands for crystallographic directions of $< 100 >$ and $< 1\bar{1}0 >$; ν_n is the effective surface tension that is generated by ion sputtering, $\nu_n > 0$; λ_n describes the tilt-dependent erosion rate; $D_n \partial^4 h/\partial \boldsymbol{n}^4$ takes into account the thermal and/or ion-induced diffusions that relax the surface instability, and $-S_n \partial^2 h/\partial \boldsymbol{n}^2$ represents the ES diffusion, which causes the surface instability. $D_{\boldsymbol{n}} > 0$ and $S_{\boldsymbol{n}} > 0$. The last term in Eq.(1) reflects a stochastic noise. In Eq.(1), the first and third terms are related to ion erosion, and are normally temperature independent, while the diffusion terms (the second and fourth terms) are sensitive to the temperature. Following the algorithm of Ref.[9], numerical integration of Eq.(1) has been conducted. Since the input data of Si(110) such as those of ν_n, λ_n, $D_{\boldsymbol{n}}$, and S_n, for running calculations are lacking, we only pursue a qualitative simulation. For simplicity, the anisotropy of

the crystallographic direction-dependent parameters has been ignored, hence the subscript $\boldsymbol{n}$ is dropped in the following. In Fig.4, four of the simulation images are presented to show the surface morphology evolution process with the increase of temperature. During the simulation, D was taken to be 2 for Figs.4(a)–(d), λ=1, ν=0.2, implying that the BH effect is still at work although it is not the main concern for the surface morphology evolution, time step =0.01, and the total time $=10^4$ steps. The system size is 256×256. From Figs.4(a)–(d), the only difference lies in S that is 0.05, 0.2, 0.4, and 0.45, respectively. The trend of change in S agrees with the rising part of the curve for ES diffusivity versus temperature (Fig.3), indicating that the change of S from 0.05 to 0.45 corresponds to the increase in sample temperature. It is seen that similar to that obtained in experiments, at and beyond a certain S, one obtains distinct dot patterns; furthermore, the larger the S, the larger the averaged dot size. Also the curve w–S (Fig.2(b)) behaves in a similar manner as the experimental w–T: that is, w increases steadily with the increase of S, and corresponding to the appearance of the distinct dot pattern, w exhibits a quick increase.

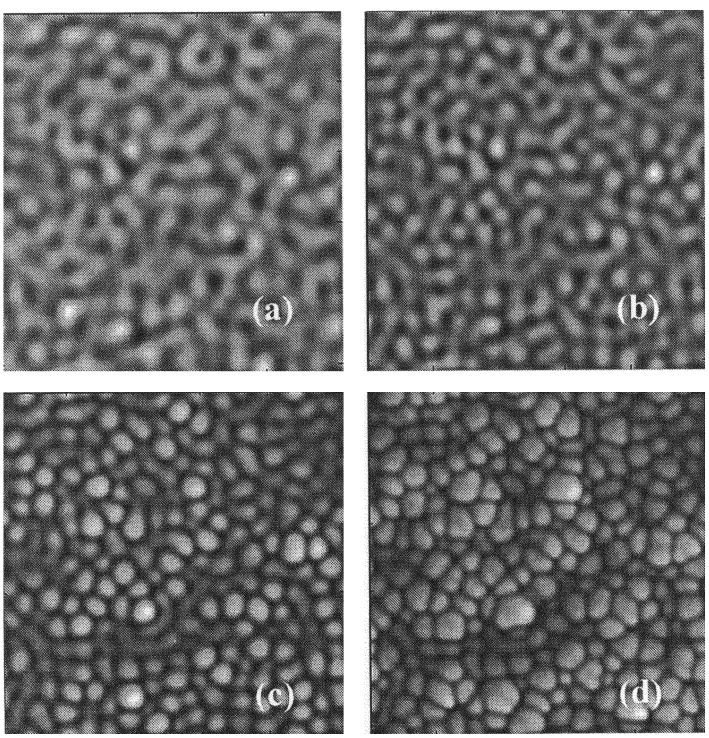


Fig.4. Simulated images. From (a)–(d), λ=1, D=2, ν=0.2, time step =0.01, and the total time $=10^4$ steps, but S= (a) 0.05, (b) 0.2, (c) 0.4, and (d) 0.45. The image system size is 256×256 for all figures.

It should be pointed out that since quantitative relationships between T–S and T–D are unable to be determined at present, how to change the value of D in a proper manner when ramping S has become a bottleneck problem in the simulation. As only a qualitative analysis is pursued in this work, to circumvent this problem so as to let the simulation continue, we have kept the value of D constant during the simulation above. This choice, although unrealistic, does not alter the qualitative conclusion: i.e., with rising T, the ES diffusion is promoted, which leads to the surface morphology evolution and the corresponding surface roughness change. The only drawback of this assumption is that the differences in S in Figs.4(a)–(d) are largely reduced since the increasing surface smoothing caused by the increase in D with rising T is ignored. For instance, if D is set at 20, reflecting the increase of thermal diffusion with rising T, in order to acquire the similar surface morphology and roughness to those of Fig.4(d), the corresponding S should be 6.8 rather than 0.45.

Although the simulated results (Figs.4(a)–(d)) agree qualitatively with the experimental ones, inconsistencies will exist regarding the morphology details.

For instance, in Figs.1(c) and (d), large size nanoholes are present, but in the simulation images (Figs.4(c) and (d)), their number is much less. Also, the dots in Figs.1(c) and (d) are more uniformly distributed in size than those in Figs.4(c) and (d). These inconsistencies indicate that the model we adopted (Eq.(1)) needs improvements. Recently, Facsko *et al*[15] found that by adding a damping term to the right side of Eq.(1), the dots from simulations can be more uniformly distributed in size. They ascribed the origin of this damping term to the re-deposition of sputtered Si atoms onto the Si substrate. However, this ascription lacks evidence so far. In this work, we do not attempt to modify the present model, but only stress that within the framework of this model, the ES effect is vital in the explanation of the observed results.

4. Conclusion

In summary, nanostructuring of Si(110) under Ar^+ ion sputtering has been investigated as a function of sample temperature. The sputtered surface morphology is reflected by a dim dot/hole pattern at temperatures lower than $\sim 600^\circ$C; at higher temperatures, the surface morphology changes to a distinct dot pattern. Also with increasing sample temperature, the surface roughness increases steadily. These temperature-dependent evolutions are caused by the ES effect. Simulation has been conducted based on a continuum dynamic model; its result agrees qualitatively with the experimental data.

References

[1] Facsko S, Dekorsy T, Koerdt C, Trappe C, Kurz H, Vogt A and Hartnagel H L 1999 *Science* **285** 1551

[2] Frost F, Schindler A and Bigl F 2000 *Phys. Rev. Lett.* **85** 4116

[3] Gago R, Vazquez L, Cuerno R, Varela M, Ballesteros C and Albella J M 2001 *Appl. Phys. Lett.* **78** 3316

[4] Habenicht S 2001 *Phys. Rev.* B **63** 125419

[5] Facsko S, Kurz H and Dekorsy T 2001 *Phys. Rev.* B **63** 165329

[6] Lu M, Yang X J, Perry S S and Rabalais J W 2002 *Appl. Phys. Lett.* **80** 2096

[7] Kalff M, Comsa G and Michely T 2001 *Surf. Sci.* **488** 346

[8] Valbusa U, Boragno C and de Mongeot F B 2002 *J. Phys.: Condens. Matter* **14** 8153

[9] Kahng B, Jeong H and Barabasi A L 2001 *Appl. Phys. Lett.* **78** 805

[10] Bradley R M and Harper J M E 1988 *J. Vac. Sci. Technol.* A **6** 2390

[11] Rusponi S, Costantini G, Boragno C and Valbusa U 1998 *Phys. Rev. Lett.* **81** 2735

[12] Politi P and Villain J 1996 *Phys. Rev.* B **54** 5114

[13] Qi L J, Li W Q, Fang Y C, Yang X J and Lu M 2005 *Chin. Phys. Lett.* **22** 431

[14] Ziegler J F (ed) 1996 *The Stopping and Range of Ions in Solids* (New York: Pergamon)

[15] Facsko S, Bobek T, Stahl A, Kurz H and Dekorsy T 2004 *Phys. Rev.* B **69** 153412